PHYSICAL REVIEW D **70,** 124022 (2004)

# Coordinate time dependence in quantum gravity

Martin Bojowald*
*Max-Planck-Institut für Gravitationsphysik, Albert-Einstein-Institut, Am Mühlenberg 1, D-14476 Potsdam, Germany*

Parampreet Singh†
*Institute for Gravitational Physics and Geometry, Pennsylvania State University, University Park, Pennsylvania 16802, USA*

Aureliano Skirzewski‡
*Max-Planck-Institut für Gravitationsphysik, Albert-Einstein-Institut, Am Mühlenberg 1, D-14476 Potsdam, Germany*
(Received 30 August 2004; published 17 December 2004)

The intuitive classical space-time picture breaks down in quantum gravity, which makes a comparison and the development of semiclassical techniques quite complicated. Using ingredients of the group averaging method to solve constraints one can nevertheless introduce a classical coordinate time into the quantum theory, and use it to investigate the way a semiclassical continuous description emerges from discrete quantum evolution. Applying this technique to test effective classical equations of loop cosmology and their implications for inflation and bounces, we show that the effective semiclassical theory is in good agreement with the quantum description even at short scales.

DOI: 10.1103/PhysRevD.70.124022 PACS numbers: 04.60.Pp, 04.25.–g, 98.80.Qc

## I. INTRODUCTION

Current knowledge of the quantum structure of space-time suggests a picture very different from the smooth classical one. Space and time are expected to be fundamentally discrete such that both change only in steps. Still, a transition between both pictures must be possible in order to understand the emergence of a classical world on large scales from the fundamental quantum world. Also for practical purposes such a transition is helpful in a semiclassical approximation. A technically and conceptually important question is where the classical picture starts to make sense or, when going to smaller and smaller scales, where it breaks down. The change of scale can happen either computationally, i.e., by looking at smaller and smaller scales in a coarse-grained approximation which can then be used, for instance, to understand the breaking or deformation of classical symmetries, or dynamically during the expansion or contraction of a universe or the collapse of matter to a black hole.

One application is the behavior of universes which on larger scales has been studied from the point of view of loop quantum cosmology [1,2] by using effective classical equations [3–6]. While the fundamental description is quantum, governed by a difference equation for the wave function [7–9], effective classical equations show the diverse cosmological effects more easily. The idea of using effective classical equations is that in semiclassical regimes they describe the position of wave packets solving the difference equation. They simplify the analysis considerably even in isotropic models and can be expected to do so even more in inhomogeneous models or the full theory. In light of the previous discussion an open question is where exactly an effective classical equation makes sense as a good approximation to the behavior of the difference equation, and where additional correction terms have to be taken into account.

This question can be answered by a direct comparison of effective semiclassical descriptions, given by ordinary differential equations, with the underlying discrete quantum evolution governed by difference equations (these difference equations may even be partial depending on the number of matter fields). However, since an ordinary differential equation is quite different from a discrete difference equation, their solutions cannot be compared directly. For such a purpose we first have to extract appropriate data from solutions of the difference equation, usually by taking expectation values, which we then compare to the classical theory or one with further corrections. (At this point one has to distinguish between ambiguities resulting from choosing how to extract the semiclassical data and outright deviations from the purely classical behavior. How this can be disentangled will be discussed later.) In this way one can see if new effects arise or in which range one can trust an effective classical equation with or without certain correction terms.

Comparing an effective theory with the underlying quantum theory is of great relevance to various issues in loop cosmology. For instance, in order to determine the starting point of inflation [3,10–12], observable signatures in cosmic microwave background [10], the validity of effective classical bounce pictures [13–17], general aspects of the approach to a classical singularity [18,19], or evolution of perturbations. If the effective theory requires further corrections from the quantum theory which can be verified by their comparison, then these correction terms in

*Email address: mabo@aei.mpg.de
†Email address: singh@gravity.psu.edu
‡Email address: skirz@aei-potsdam.mpg.de

 

principle can leave an observational signature which can be used to verify loop quantum cosmology.

A particularly striking difference between the classical and the quantum theory is the issue of time. A common understanding which works in both cases is that of relational time, where time is not an external, absolute parameter but encoded in the relative change between different degrees of freedom [20–22]. However, this concept is difficult to use explicitly, and so classically one employs the space-time picture where time is just a gauge coordinate. Thus, this time coordinate has no invariant physical meaning, but nevertheless provides a helpful intuitive understanding of a given gravitational system. From the Hamiltonian point of view, this time coordinate is the gauge parameter for orbits generated by the Hamiltonian constraint. In this way, coordinate time is related to the second effect of a first class classical constraint, namely, that of generating a gauge transformation in addition to restricting fields to the constraint surface.

In a canonical quantum theory the situation is different because in the Dirac procedure to solve first class constraints there is only one step by requiring physical states to be annihilated by the quantum constraints, which then are automatically gauge invariant. In systems with a Hamiltonian constraint, physical states are thus timeless, which has led to the name ''frozen formalism.'' As we will discuss below, the two steps familiar from the classical procedure can easily be disentangled also in a quantum procedure to solve the constraints, in particular, if the technique of group averaging [23] is used. Physical states can then be represented in an evolving manner, depending on the gauge choice via the lapse function. We emphasize that our notion of evolution in time as used here is with respect to coordinate time and not physical time. We call this coordinate time-dependent family of states a ''state-time'' in order to indicate that classical space in a space-time has been replaced by a quantum state, while time remains classical. At a given time parameter of the state-time the constraints will not be satisfied, but the whole state-time represents a physical state, which can be reconstructed by integrating over time, in a well-defined way.

As a practical application we develop a scheme to decide the domain of validity of an effective semiclassical description and whether in some regimes it requires further correction terms. For that, we compare the expectation value of, e.g., the volume in a given state-time with the volume obtained from the classical theory (or with an effective theory including further corrections). The correction terms can be derived by computing the expectation value of the Hamiltonian constraint operator in a coherent state and expanding around the classical expression [24,25]. There are diverse sources of deviations in the case of nonlinear constraints which can be studied analytically or numerically: First, there are the usual Ehrenfest statements about the relation between classical and quantum equations of motion for expectation values. In addition there are choices related to choosing an initial semiclassical state, and the way the constraints are violated at fixed coordinate times. Finally and most importantly, there are genuine quantum gravity corrections whose implications can give rise to new physical effects. The latter imply the modifications we want to include in effective classical equations.

As we will see, it is possible to disentangle these effects at least qualitatively. The resulting modifications to classical behavior can then be compared to known analytical results, as is done here for inflationary behavior and bounces, or used to suggest new effects. In the next section we recall the group averaging procedure which will be followed by a brief discussion of the issue of introducing coordinate time in this context. In Sec. IV we will present a way to implement this idea numerically and study examples of universes with a cosmological constant or dust as matter. We will show that, both for inflation and bounces, the effective semiclassical theory which incorporates modified geometrical densities is in good agreement with discrete quantum evolution till very small scales. This proves that effects derived from the effective semiclassical theory capture to a large extent the true nature of quantum space-time. Here we focus on describing the way our technique can prove useful in testing a semiclassical theory, leaving a more detailed study for future work.

## II. GROUP AVERAGING

We will discuss here only systems with a single constraint which we mostly think of as a Hamiltonian constraint generating coordinate time. In an isotropic cosmological model the constraint itself will be the Friedmann equation, and the evolution equation it generates is the Raychaudhuri equation plus equations for matter fields such as the Klein-Gordon equation for a scalar. After quantizing we obtain the constraint operator which annihilates physical states, and all evolution would have to be extracted from physical states in a relational way.

A simple method to implement a constraint on quantum states is as follows. Consider the action of the constraint operator $\hat{C}$ on a given nonphysical state interpreted to promote a change in gauge parametrized by a real parameter $\lambda$,

$$\hat{C}|\varphi_\lambda\rangle = i\frac{\mathrm{d}}{\mathrm{d}\lambda}|\varphi_\lambda\rangle. \tag{1}$$

Obviously $|\varphi_\lambda\rangle$ is not annihilated by the operator $\hat{C}$ unless $|\varphi_\lambda\rangle$ is independent of $\lambda$, i.e., gauge invariant. To achieve $\lambda$ independence we can average the state $|\varphi\rangle \equiv \int \mathrm{d}\lambda|\varphi_\lambda\rangle$ such that

$$\hat{C}|\varphi\rangle = \int \mathrm{d}\lambda \hat{C}|\varphi_\lambda\rangle = i\int \mathrm{d}\lambda \frac{\mathrm{d}}{\mathrm{d}\lambda}|\varphi_\lambda\rangle, \tag{2}$$

which in the case of compact symmetry orbits or suitable

boundary conditions in the noncompact case vanishes identically. In conclusion, we can get a solution to our constraint by averaging the nonphysical state over the symmetry group: $\int \mathrm{d}\lambda|\varphi_\lambda\rangle$. This is in fact not new because the solution to our equation for a state $|\varphi_\lambda\rangle$ is given by

$$|\varphi_\lambda\rangle = e^{-i\lambda\hat{C}}|\varphi_0\rangle \tag{3}$$

and the invariant state is

$$\int \mathrm{d}\lambda e^{-i\lambda\hat{C}}|\varphi\rangle, \tag{4}$$

which is nothing else than the group averaging map [23] into the physical Hilbert space.

As examples we consider different cases in which the method works with different success. The simplest case would be to consider the constraint $\hat{P}_\theta|\varphi\rangle = 0$ which imposes rotation invariance on a two dimensional system with angular coordinate $\theta$. Then, by following the prescription presented above we replace the equation

$$\langle\theta|\hat{P}_\theta|\varphi\rangle = i\partial_\theta\varphi(\theta) = 0 \tag{5}$$

with a Schrödinger-like equation. The constraint then acts on nonphysical states by

$$i\partial_\theta\varphi_\lambda(\theta) = i\partial_\lambda\varphi_\lambda(\theta) \tag{6}$$

with general solution

$$\varphi_\lambda(\theta) = \varphi(\lambda + \theta). \tag{7}$$

Physical states are thus given by

$$\varphi = \int_0^{2\pi} \mathrm{d}\lambda\varphi(\lambda + \theta) = \int_0^{2\pi} \mathrm{d}\lambda\varphi(\lambda), \tag{8}$$

where any $\theta$ dependence is removed.

We can also consider the noncompact case by using the translation generator $\hat{P}_x$ with exactly the same calculations (except that allowed functions $\varphi$ have to be restricted to a suitable set for the $\lambda$ integration to exist, similarly to selecting an appropriate subspace of the kinematical Hilbert space for group averaging). For a more general example let us consider the operator $\hat{C} = a\hat{X}\hat{P} + b$ to follow the strategy above, i.e., use the operator to generate transformations of an arbitrary state, and then solve the resulting partial differential equation. In this case the equation becomes

$$(axi\partial_x + b)\varphi_\lambda(x) = i\partial_\lambda\varphi_\lambda(x) \tag{9}$$

with solution

$$\varphi_\lambda(x) = e^{(ib/2)[(1/a)\ln(x)-\lambda]} f(\ln(x)/a + \lambda). \tag{10}$$

Then, in order to realize the $\lambda$ integration we Fourier transform $f(\frac{1}{a}\ln(x) + \lambda)$, which is possible only for $a$ real: $f(u) = (2\pi)^{-1}\int_{-\infty}^{\infty}\mathrm{d}\omega e^{-i\omega u}\tilde{f}(\omega)$. Moreover, we commute the $\lambda$ and $\omega$ integrations,

$$\int_{-\infty}^{\infty}\mathrm{d}\lambda\varphi_\lambda(x) = e^{i(b/2)(1/a)\ln(x)}\int_{-\infty}^{\infty}\frac{\mathrm{d}\omega}{2\pi}e^{-i\omega(1/a)\ln(x)}\tilde{f}(\omega) \times \int_{-\infty}^{\infty}\mathrm{d}\lambda e^{-i[\omega+(b/2)]\lambda}. \tag{11}$$

Here, the integral in $\lambda$ would diverge for arbitrary complex $b$ and we get a solution for the constraint only if it is real. After integrating over $\lambda$ and $\omega$ we obtain $\varphi(x) = ce^{i(b/a)\ln(x)}$, which can be checked to satisfy our constraint. If $b \notin \mathbb{R}$, the final integration diverges which means that we are not allowed to commute the integrations. Moreover, in this case we would have to choose appropriate fall-off conditions for $f$.

Whether or not we are using a self-adjoint constraint operator has significance for the physical inner product, which we are not considering here. Still, adjointness properties also play a role at the level of solving the constraint, as the following example given by $\hat{C} = \partial/\partial x$ demonstrates. Now we have to solve the equation

$$\partial_x\varphi_\lambda(x) = i\partial_\lambda\varphi_\lambda(x),$$

which is done by any arbitrary function $\varphi_\lambda(x) = \varphi(\lambda + ix)$ depending only on $\lambda + ix$. Integrating over $\lambda$ to compute a physical state is now done along a line shifted vertically by the amount $x$ in the complex plane, where we interpret solutions $\varphi_\lambda(x)$ as holomorphic functions on the complex plane with coordinate $z = \lambda + ix$. The result will be independent of $x$ only if $\varphi$ satisfies appropriate fall-off conditions and does not have residues. Both properties together cannot be satisfied for nonzero functions since, owing to Liouville's theorem any bounded entire function is constant. Thus, any function for which the $\lambda$ integrations exist must have poles on the complex plane such that the averaging procedure does not lead to constant functions of $x$, as expected for this constraint, but only to locally constant ones.

While the averaging can be defined even for non-self-adjoint constraints, from the numerical point of view self-adjointness of the constraint operator is essential. Nonreal eigenvalues would imply exponentially growing modes in solutions to the differential equation which lead to numerical instabilities.

## III. COORDINATE TIME

Quantum gravity in the perspective of canonical quantization arises as a constrained system which gives rise to the well-known Wheeler-DeWitt equation instead of a Schrödinger-like equation. Nowadays canonical quantum gravity is usually formulated with Ashtekar variables and it is possible to realize the constraint algebra on a well-defined kinematical Hilbert space [26–30]. The Gauss and diffeomorphism constraints can be solved by group averaging [26], but discussions about the correct Hamiltonian constraint are not settled yet [27,30–32]. Also the issue of the physical inner product and how to

use the solution space to the Hamiltonian constraint are almost completely open in the full theory. After reducing to symmetric models [33], the Hamiltonian constraint simplifies and can often be treated explicitly. Even in the simplest cosmological models the physical inner product is not yet understood, but since the spatial volume can be used as internal time in a cosmological situation the problem of time does not play a role. In all these cases there is a Hamiltonian constraint whose gauge parameter classically corresponds to coordinate time, and it is our aim to discuss how such a parameter can appear with this interpretation in quantum theory. We emphasize that, as a general problem, this is much simpler than the problem of time where time is understood as a physical parameter valid for the full quantum theory. In contrast, we are interested in formulating the quantum theory in a parametrized way, with a new nonphysical coordinate time parameter. Moreover, this parameter is expected and intended to make sense only in semiclassical regimes. This will be discussed in more detail in the Conclusions, making use of what we learned in the examples.

As discussed before, the group averaging procedure to solve constraints can be split into two steps which roughly correspond to the two classical steps of restricting to the constraint surface and factoring out by the gauge orbits. The correspondence is not perfect, however, since one single member $\varphi_{\lambda_0}$ of a family $\{\varphi_\lambda\}_{\lambda\in\mathbb{R}}$ of states exhibiting the gauge parameter, which we call state-time in the case of a gravitational system, is not a solution to the quantum constraint, while a classical gauge orbit can completely lie within the constraint surface. Even in a semiclassical regime this would lead to deviations between the classical and quantum behavior since the constraints are always violated when the gauge parameter is exhibited. Still, as an approximation and a heuristic tool the gauge dependent family of states can be very useful. In particular, for the Hamiltonian constraint of a gravitational system this allows us to describe the quantum dynamics approximately (in the sense that the constraint is not imposed exactly for otherwise the state-time would have to be time independent) with reference to a coordinate time, which justifies the use of effective classical equations of motion.

Taking into account possible choices of lapse functions, which after quantizing can be operators if $N$ depends on $t$ via kinematical degrees of freedom [such as $N(t) = a(t)$, which is used when transforming from proper time to conformal time in an isotropic model], we arrive at

$$\hat{N}\,\hat{H}\,|\Psi_t\rangle = i\frac{\mathrm{d}}{\mathrm{d}t}|\Psi_t\rangle \tag{12}$$

as the evolution specified by the Hamiltonian constraint operator.

The condition that the Hamiltonian constraint has to annihilate physical states emphasizes the fact that physics does not depend on (coordinate) time. Correspondingly, Eq. (12), which is directly related to a choice of time through a Schrödinger equation on nonphysical states, and the state-time $|\Psi_t\rangle$ solving it are in fact not unique because we can fix the gauge freedom in different ways by making different choices of the quantized version $\hat{N}$ of the lapse function.

If we were interested in completing the group averaging we would have to integrate the state-time over $t$ in order to arrive at a physical state. However, just as the classical space-time picture, which we are interested in here, arises only when gauge orbits parametrized by coordinate time $t$ are not factored out, we have to refrain from performing this final step and instead work only with the state-time. In principle, with much effort one can always remove all gauge dependence, classically by factoring out gauge and in quantum theory by integrating over the gauge group, but physical intuition is best developed in a (coordinate) time-dependent picture. Nevertheless, we think that the discussion of group averaging justifies our use of the state-time and the following applications.

## IV. APPLICATIONS

For semiclassical physics it is very convenient to have an explicit coordinate time parameter since classical intuition is based on the space-time picture. In principle it is also possible to work with internal times both at the quantum and classical level, but it comes with much more technical effort. In the case of loop quantum cosmology, in fact, most recent phenomenological applications [3,6,10–19] are based on effective classical equations [3,4], which are differential equations in coordinate time and implement the main nonperturbative quantum effect [34,35] in matter Hamiltonians [36]. Direct studies of the underlying difference equations, on the other hand, are more complicated [37–41].

These equations show the main qualitative effects that have to be expected from the loop quantization at a more intuitive level. For more quantitative applications, however, it is important to see to which degree they provide an approximation (in the sense discussed in the Introduction) to the quantum behavior and whether in some regimes additional correction terms have to be taken into account. One way of evaluating these correction terms, for instance, is to compute the expectation value of the constraint operator in a coherent state [24,25]. This results in the classical constraint together with correction terms, and thus corrected equations of motion for, e.g., the scale factor. The present paper suggests an alternative procedure, which is one step closer to the quantum theory. Using the quantum coordinate time picture, we can evolve the state first within the quantum theory, and then compute the expectation value of, e.g., the volume operator which also gives us the time dependence of the scale factor. Both procedures are approximations to the quantum dynamics: In the first case one uses kinematical coherent

states to compute the expectation value, while in the second case coordinate time is introduced which, as explained above, is not exact in quantum theory. In both cases, however, the Hamiltonian constraint is used and implemented at least partially: The first case imposes a classical constraint with quantum corrections, while in the second the quantum constraint is used to evolve states, which then could be averaged if we are interested in the physical state.

In a sense, the procedures differ by a commutation of evolving and translating from quantum to classical behavior (by taking expectation values). We either take the expectation value of the constraint first (in a kinematical coherent state) and then determine the evolution in a classical manner, or we first evolve a kinematical state with quantum operators and then determine classical quantities from expectation values in the resulting, time-dependent states. It is not guaranteed that the two different steps in fact commute, which leads to differences between the two procedures. In simple models, however, both ways of determining the dynamics can be implemented at least numerically and then compared with each other. We will demonstrate this in what follows, leaving a more detailed investigation with precise statements of ranges of applicability and of the necessity of additional correction terms for future work.

### A. Numerical implementation

In isotropic loop quantum cosmology for a flat model, the Hamiltonian constraint operator is given by [8,24]

$$(\hat{H}_0\tilde{\psi})_\mu = (V_{\mu+5} - V_{\mu+3})\tilde{\psi}_{\mu+4} - 2(V_{\mu+1} - V_{\mu-1})\tilde{\psi}_\mu + (V_{\mu-3} - V_{\mu-5})\tilde{\psi}_{\mu-4} + \tfrac{8}{3}\pi G\gamma^3\ell_{\mathrm{P}}^2\mathrm{sgn}(\mu)\hat{H}_{\mathrm{matter}}(\mu)\tilde{\psi}_\mu$$

acting on a wave function $\tilde{\psi}\colon \mathbb{R} \to \mathbb{C}$ supported on eigenspace of the triad operator $\hat{p}$. The coefficients are given in terms of the volume eigenvalues $V_\mu = (\frac{1}{6}\gamma\ell_{\mathrm{P}}^2)^{3/2}|\mu|^{3/2}$, with the Barbero-Immirzi parameter $\gamma = 0.238$ [42,43] as it follows from calculations of black hole entropy [44,45], and $\hat{H}_{\mathrm{matter}}(\mu)$ is the matter Hamiltonian which we will choose later.

Since only labels with distances of four apart are involved, we introduce $4m := \mu$ with integer $m$ (see also [46] for this restriction) and write the operator as

$$(\hat{H}_0\psi)_m = (v_{m+5/4} - v_{m+3/4})\psi_{m+1} - 2(v_{m+1/4} - v_{m-1/4})\psi_m + (v_{m-3/4} - v_{m-5/4})\psi_{m-1} + \tfrac{8}{3}\pi G\gamma^3\ell_{\mathrm{P}}^2\mathrm{sgn}(m)\hat{H}_{\mathrm{matter}}(4m)\psi_m,$$

with $\psi_m := \tilde{\psi}_{4m}$ and $v_m := V_{4m}$. This operator will have to be symmetrized to $\hat{H} := \frac{1}{2}(\hat{H}_0 + \hat{H}_0^\dagger)$ for the numerical implementation of coordinate time to be stable. (Alternatively, we can choose a lapse function $N(t) = a(t)$, corresponding to conformal time, and quantize such that $\hat{N}$ has eigenvalues proportional to $V_{\mu+1} - V_{\mu-1}$. The resulting operator $\hat{N}\hat{H}_0$ would be symmetric without reordering $\hat{H}_0$, but since the lapse function and its quantization vanish for $a = 0$, the quantum behavior around $\mu = 0$ will be problematic.)

For numerical purposes we need to restrict the operator to finite lattices $\mathcal{L}_{m_c,N} := \{n \in \mathbb{Z} : m_c - N/2 < m \leq m_c + N/2\}$ of size $N$ and centered at $m_c$, such that it will be represented by a tridiagonal $N \times N$ matrix $H_{ij}$ with $H_{ij} = 0$ for $j > i + 1$ or $i > j + 1$,

$$H_{ii} = -2(v_{m_c-N/2+i+1/4} - v_{m_c-N/2+i-1/4}) + \tfrac{8}{3}\pi G\gamma^3\ell_{\mathrm{P}}^2\mathrm{sgn}(m_c - \tfrac{1}{2}N + i)\hat{H}_{\mathrm{matter}}(m_c - \tfrac{1}{2}N + i) \tag{13}$$

and

$$H_{i,i+1} = H_{i+1,i} = \tfrac{1}{2}(v_{m_c-N/2+i+5/4} - v_{m_c-N/2+i+3/4} + v_{m_c-N/2+i+1/4} - v_{m_c-N/2+i-1/4}). \tag{14}$$

The above splitting of the Hamiltonain matrix into diagonal and off-diagonal parts is done purely for numerical convenience. We now introduce the coordinate time parameter $t$ and solve

$$H \cdot \psi_t = i\frac{\mathrm{d}}{\mathrm{d}t}\psi_t \tag{15}$$

numerically. The solution to the differential equation (15) is then given by

$$\psi_t = \exp(-itH) \cdot \psi_{\mathrm{in}}$$

with an initial state $\psi_{\mathrm{in}} \in \mathbb{C}^N$. The function $\psi_t$ can then be used to compute time-dependent expectation values.

### B. Examples

As examples of our technique, we would now investigate various cases of matter Hamiltonian and compare the effective semiclassical theory with the evolution determined by quantum difference equations. We first consider the case where matter Hamiltonian is just a cosmological constant and the scale factor is the sole degree of freedom. Unlike with an internal time evolution, for which no other degree of freedom besides internal time $a$ would be left, this still allows us to have a nontrivial evolution of $a$ in coordinate time $t$. This example is then followed by examples of inflation and bounce with inclusion of matter (dust) in the analysis which signifies the role played by effective densities in a good semiclassical description.

The total Hamiltonian is given by

$$\frac{3}{2}a\dot{a}^2 - 8\pi G H_{\mathrm{matter}} = 0, \tag{16}$$

which leads to the Friedmann equation

$$\frac{\dot{a}^2}{a^2} = \frac{16\pi G}{3}\rho(a). \tag{17}$$

In our first example we take $\rho(a) = \Lambda$ and later we will consider the classical dust density $\rho(a) = M/a^3$. In general, there are two qualitatively different kinds of modifications which bring the behavior of effective cosmological equations closer to that of the quantum theory, which we will study in what follows. First, by nonperturbative effects the geometrical density $a^{-3}$ in the matter Hamiltonian density is replaced by a function which is finite and does not diverge at small $a$. The precise form of the function will be discussed below. Secondly, there are perturbative corrections in the gravitational part $\dot{a}^2/a^2$ of the constraint which appear as additional terms on the left-hand side of the Friedmann equation. We will mainly discuss one such term, which includes effects of the spread of a wave packet in the effective classical framework.

### *1. Effective classical behavior: Cosmological constant*

In order to compare the evolution given by an effective theory and the quantum difference equation we first have to choose an initial state $\psi_{\rm in}$. This state should be peaked on a specified classical volume, together with an extrinsic curvature which follows from the volume and the classical Hamiltonian constraint to which we compare the quantum evolution. In principle, one can use any suitable state as an initial state; however, for simplicity we will use a Gaussian

$$\psi_{{\rm in},k} = \exp\left[-\frac{(k-N/2)^2}{4\sigma^2} + 2i(k-N/2)c_0\right]$$

in what follows. Here the isotropic connection component $c_0$ is related to extrinsic curvature by $c = -\gamma\dot{a}/2$. It is determined from the peak scale factor $a_0 = \sqrt{(2/3)\gamma\ell_{\rm P}^2|m_c|}$[1] by the constraint $-6c_0^2a_0 + 8\pi G\gamma^2 H_{\rm matter}(a_0) = 0$. (At this point the classical equations to be compared with enter. If correction terms are included, as will be done later, the value of $c_0$ changes and so does the quantum evolution of the new initial state.) Nevertheless, the explicit choice has an influence on the evolution such as the degree of spreading of the wave packet. Numerically, a choice leading to less spreading will allow the evolution to be reliable for a longer period of time since the boundary values will remain small longer and finite size effects will set in later.

For our purpose, comparing the quantum evolution with classical equations, the choice of initial wave packet is not that important since it is sufficient to know the evolution for limited amounts of time only. We will not be able to compare whole solutions as functions of time in this way, but since the classical equations and also the corrected ones are local in time we can study deviations. One can then decide which correction terms are needed to describe the local change in volume following from the quantum evolution.

A quantitative statement about the deviations is complicated by the fact that the quantum evolution is not uniquely related to a classical expression. One can take expectation values and compare with the classical functions, but due to the spread of the probability distribution the result depends on whether we take, e.g., the expectation value

$$\langle\hat{V}\rangle(t) = \|\psi_t\|^{-2}\sum_{k=1}^{N} v_{m_c-N/2+k}|\psi_{t,k}|^2 \tag{18}$$

of the volume operator or that of the scale factor operator $\hat{a} = \hat{V}^{1/3}$ and the cubic power afterwards.

Using these ingredients we compute the volume for the quantum equation (15) and the classical theory [Eq. (17)]. Classically, we have $V = a^3$, but this relation will certainly not be satisfied for the expectation values of $\hat{V}$ and $\hat{a}$ once the spread of the wave function becomes large. In Fig. 1, we have shown the behavior of expectation values of the volume operator $\hat{V}$ (+) and that evaluated from $\hat{a}$ (×). These are compared with the volume calculated from the classical theory (dashed curve). As is clear, the classical theory gives a very good approximation to the underlying evolution from the difference equation. However, due to spread of the wave packet some discrepancy occurs for late times. This can also be noticed in the evolution of the wave packet which is shown in Fig. 2. Comparing the two different ways of computing volume expectation values shows

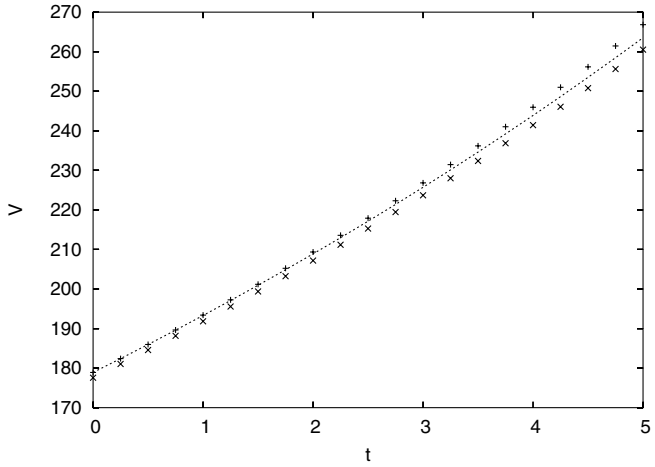


FIG. 1. Expectation value of the volume (+) compared to the effective solution $V(t)$ (dashed curve) and the volume $\langle\hat{a}\rangle^3(t)$ computed from the expectation value of the scale factor (×) for the case of cosmological constant. The initial peak of the coherent state is chosen around $m_c = 200$ with $\sigma = 20$ and $N = 500$. We take $\Lambda = 10^{-3}$.

[1]The loop quantization of the symmetry reduced cosmological model from the full theory is done in such a way that the scale factor as used here (which is related to the cubic root of the volume of the fiducial cell necessary to define symplectic structure) is invariant to its conventional rescaling freedom in classical cosmology. For details see Ref. [24].

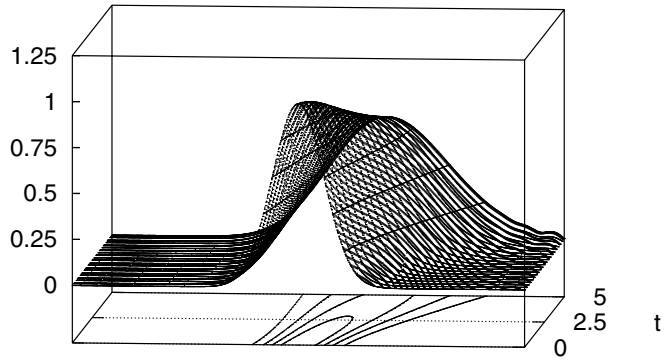


FIG. 2. A spreading wave packet for $\Lambda = 10^{-3}$, as in Fig. 1. At the back of the right-hand side one can see small oscillations building up when the wave reaches the boundary. The vertical axis shows the magnitude of the normalized wave function, which starts as a Gaussian at the front and evolves to the back.

that the discrepancies do not result from new physical effects but only reflect the ambiguous way of relating expectation values to classical behavior.

In general, departures between expectation values of the volume operator and classical values can have several reasons. Besides approximations used in the method to solve the constraint, there are quantum effects which we are most interested in here. They can be divided into two classes: the first one arising from small-scale or high-curvature effects in quantum operators, the second one coming from the fact that we have an evolving wave packet rather than a sharp classical point. Both effects can be included into effective classical equations, but in the second case it is not always clear if modifications to the classical behavior are a consequence of having chosen a bad initial state or a physical effect related to the evolution of spread, asymmetry, and other deformations in profile of the probability distribution.

In order to quantify this, one can evaluate the skewness of the wave function as it evolves. The skewness which is initially zero for the Gaussian coherent state describes the asymmetry of the wave packet and is given in terms of various expectation values of powers of $\hat{p} = \hat{V}^{2/3}$ as

$$s = \frac{1}{\tilde{\sigma}^3}[\langle\hat{p}^3\rangle - 3\langle\hat{p}\rangle\langle\hat{p}^2\rangle + 2\langle\hat{p}\rangle^3], \tag{19}$$

where $\tilde{\sigma}$ is the standard deviation $(\langle\hat{p}^2\rangle - \langle\hat{p}\rangle^2)^{1/2}$ which initially is given by $\tilde{\sigma}_{\rm in} = \frac{2}{3}\gamma\sigma$. (We use $\hat{p}$ in order to define skewness because it is the isotropic component of the densitized triad, which is basic in loop quantum gravity. Eigenvalues of $\hat{p}$ are proportional to $\mu$ or $m$ such that the skewness is computed for the variable in the wave function.) It is clear from Fig. 3 that the initial Gaussian wave packet gets skewed with time and deforms, but the deformation remains small such that the main parameters characterizing the wave packet in the cases studied here are only its expectation value and spread.

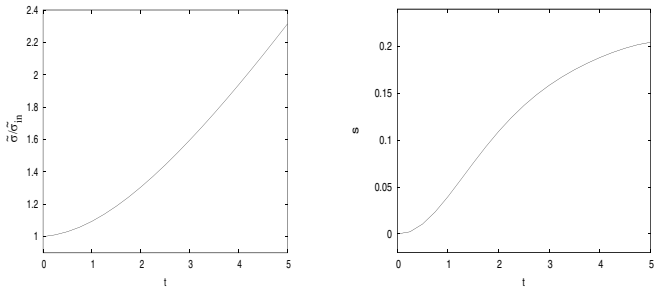


FIG. 3. Growth of standard deviation $(\tilde{\sigma}/\tilde{\sigma}_{\rm in})$ and skewness $(s)$ for the cosmological constant case studied in Fig. 1. The coherent state remains almost peaked over the classical value due to small growth in skewness.

The evolution of skewness with time reflects the fact that the coherent state is no longer peaked at its classical value, which is one cause of departure between quantum and classical curves. Figure 3 shows the spread of the wave function with respect to its initial value. A symmetric spreading would give an evolved coherent state still peaking at classical values at late times for the operator $\hat{a}^2$ corresponding to the discrete argument $m$ of the wave function. The significance of small growth in skewness for the time scale of interest is that the probability distribution of the wave function remains peaked close to the classical volume. Moreover, since the quantized volume and scale factor are given by powers of $m$ different from one, they do not follow the classical curve exactly, their difference increasing with increasing spread and skewness.

This discussion shows that a comparison between quantum and (effective) classical behavior cannot be done arbitrarily precisely because of the unsharp nature of quantum wave packets. To determine the level up to which a comparison is reliable we have different techniques as illustrated in this case. The spread of the wave packet and its deformation can be computed and plotted such that a strong growth signals stronger departures. Similarly, plotting expectation values of different powers shows a window in which the classical curve has to be expected if there would be no quantum modifications to the equations of motion. As we will see in the following examples, effects from such quantum modifications are much stronger such that they can easily be separated from simple spread effects.

### *2. Accelerated expansion*

In the previous subsection on cosmological constant we showed that evolution extracted from the quantum difference equation by introduction of coordinate time agrees well with the evolution determined classically. Now we will study the case of a dust Hamiltonian by introducing the modification to geometrical density in the Friedmann equation (17). This modification to geometrical density is a novel prediction of loop quantum cosmology at short scales and has led to various interesting applications [3–

19]. The main new ingredient is then given by a nonperturbative modification to the classically diverging density $a^{-3}$ (which has been derived in [35] and is based on expressions of the full theory [36]) relevant at small volumes. If a matter Hamiltonian has a density term then such modifications would enter dynamics and change the behavior at small-scale factors. For example, the Hamiltonian for a massive scalar field $\phi$ is given by

$$H_\phi(a) = \frac{1}{2}a^{-3}p_\phi^2 + a^3V(\phi), \tag{20}$$

with momentum $p_\phi$ and potential $V(\phi)$. This Hamiltonian in loop quantum cosmology is modified to

$$H_\phi(a) = \frac{1}{2}d_{j,l}(a)p_\phi^2 + a^3V(\phi), \tag{21}$$

where $d_{j,l}$ is the modified geometrical density given by

$$d_{j,l}(a) = a^{-3}D_l(3a^2/\gamma j\ell_{\mathrm{P}}^2), \tag{22}$$

where

$$D_l(q) = q^{3/2}\Big\{\frac{3}{2l}\Big(\frac{1}{l+2}[(q+1)^{l+2} - |q-1|^{l+2}] - \frac{q}{l+1}[(q+1)^{l+1} - \mathrm{sgn}(q-1) \times |q-1|^{l+1}]\Big)\Big\}^{3/(2-2l)} \tag{23}$$

and $j$ is a quantization ambiguity parameter (a half-integer) [35]. There is another ambiguity parameter $0 < l < 1$ [2], which is more restricted by full loop quantum gravity and is usually taken as $l = 3/4$. For very small $a \ll \sqrt{j}\ell_{\mathrm{P}}$, $d_{j,l}(a)$ behaves as a positive power of $a$,

$$d_{j,l}(a) \sim \Big(\frac{3}{l+1}\Big)^{3/(2-2l)}(3a^2/\gamma\ell_{\mathrm{P}}^2 j)^{3(2-l)/(2-2l)}a^{-3}, \tag{24}$$

i.e.,

$$d_j(a) := d_{j,3/4}(a) \sim (\tfrac{12}{7})^6(\tfrac{1}{3}\gamma\ell_{\mathrm{P}}^2 j)^{-15/2}a^{12}. \tag{25}$$

This is the main ingredient for effective classical equations with the most dramatic effects, and the methods developed here allow us to put this term in effective equations on a more solid footing. In order to avoid numerical complications related to the additional degree of freedom $\phi$ we use a dust model and employ the same effective density for its energy density $\rho(a) = M/a^3$. We emphasize that for dust this modification to the matter density is not the one most naturally expected from loop quantum gravity. Rather, in loop quantum gravity the matter *Hamiltonian* is primary and will be quantized. Since this is a constant $M$ for dust, there would be no modifications of this kind at all to the classical equations. We use the modification (which can also be interpreted as arising from an additional quantization ambiguity [11,47]) here to model the kinetic term of a scalar field Hamiltonian, and in order to study the implications of effective densities.

To that end we replace the classical matter energy density for dust, $\rho(a) = M/a^3$ with a constant $M$, by $\rho(a) = Md_{j,l}(a)$ and study the evolution as determined by (15) and the effective theory. Note that unlike the case with a cosmological constant, the effective theory is different from the classical one [in which $\rho(a) = M/a^3$] due to the introduction of a modified geometrical density. To see the differences between the two (which also highlights the role of introducing $d_{j,l}$) let us first compare the volume expectation values from (15) with the classical theory. We have shown the results in Fig. 4. It is interesting to see the way the effective density modifies the quantum dynamics given by difference equations. As is clear from the plot, the classical theory does not match the quantum description which indicates that the volume expectation value increases more strongly than the classical solution, which unlike in Fig. 1 is not an effect of a spreading wave packet or skewness. Figure 5 shows that spreading and skewness of the wave packet are not large. This is also depicted in Fig. 6 showing that the wave packet does not spread strongly during the displayed evolution.

From Fig. 4 it can be seen that the expectation value of the volume operator agrees better with the cubic power of the expectation value of the scale factor than with the classical solution. This is another sign that the modified dynamics is responsible for the deviations, rather than just change in shape of the wave packet during evolution. However, Fig. 4 does not tell us decisively how well the expectation values would agree with modified classical dynamics. A hallmark of the effective density $d_j(a)$ is

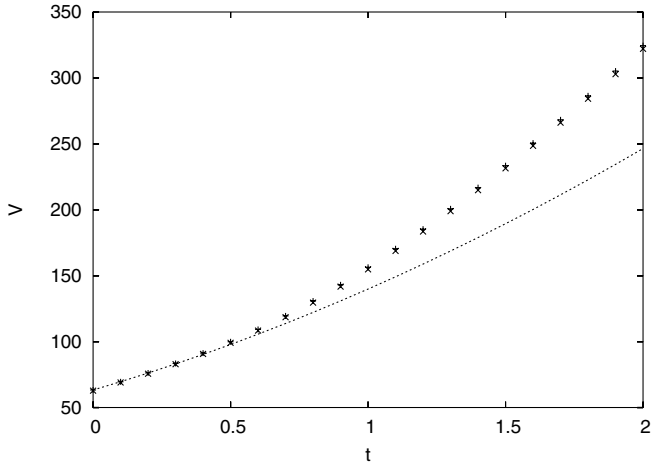


FIG. 4. Expectation value of the volume (+) compared to the classical solution $V(t)$ (dashed curve) and the volume computed from the expectation value of the triad ($\times$) for dust with $M = 10$ and an initial peak around $m_c = 100$ ($N = 1000$, $\sigma = 20$). The ambiguity parameter $j$ for the effective density is $j = 400$, such that the density peaks at $m_* \approx j/2 = 200$ corresponding to a volume $V_* = (2\gamma\ell_{\mathrm{P}}^2 m_*/3)^{3/2} \approx 180\ell_{\mathrm{P}}^3$, which is reached around $t = 1.1$.

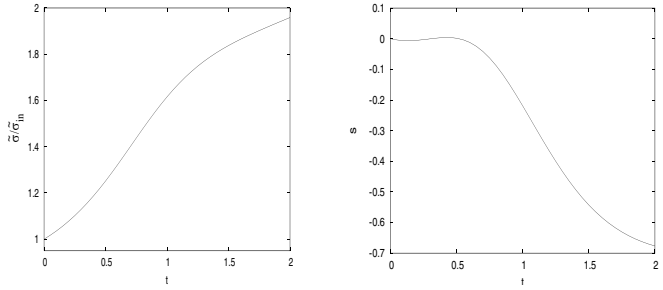


FIG. 5. The evolution of standard deviation and skewness for the case in Fig. 4. The spread increases most strongly in the inflationary regime ($t < 1.1$), while the wave packet is skewed stronger during unaccelerated expansion.

that it implies inflation (accelerated expansion) when inserted into the classical equations and when the scale factor is below the peak value. In fact, the expectation values in Fig. 4 increase more strongly than the classical solution, but in the range $0 < t < 1.1$, where we are below the peak, deviations are small.

It is much more illuminating to plot time derivatives, or rather difference quotients from the numerically obtained data, and compare with the classical behavior. Figure 7 shows that, in fact, the derivative of the scale factor increases when $t < 1.1$, i.e., below the peak of $d_j(a)$, and thus accelerates in agreement with the expectation. This figure also shows that classical description completely fails to capture the variation of scale factor with time as dictated by quantum theory.

So far we have seen that the quantum evolution differs significantly from the classical one and, in particular, leads to accelerating scale factor expectation values and thus inflation. Now we turn our attention to the effective theory where $a^{-3}$ in the matter density is replaced by $d_j(a)$. We thus obtain a modified classical description which, as we will show, agrees quite well with evolution determined by difference equations.

In order to check the effective density more directly we compare the expectation values to numerical solutions of this effective classical equation with the matter density replaced by $Md_j(a)$. The result is shown in Fig. 8. On

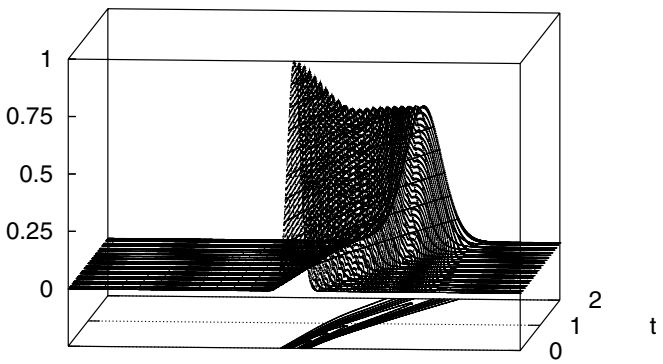


FIG. 6. A spreading wave packet $|\psi_{t,i}|$ for the evolution shown in Fig. 4.

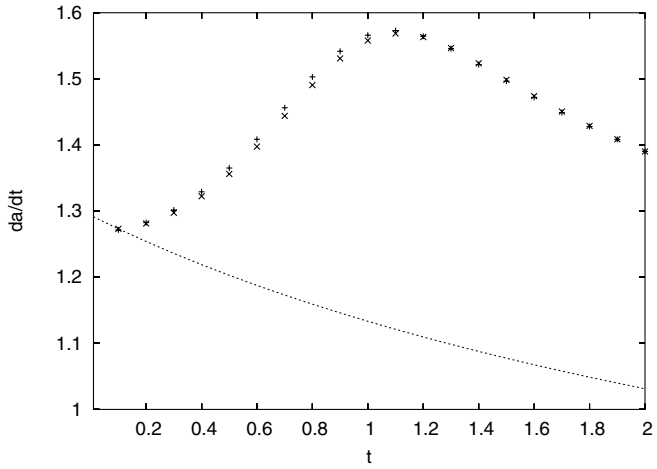


FIG. 7. Time derivative of scale factors (+ corresponds to those computed from volume expectation value and × refers to those of scale factor expectation values) plotted in Fig. 4. The dashed curve shows the classical curve. The classical description does not match the evolution from quantum theory.

comparison with Fig. 4, it is clear that the effective theory matches the quantum evolution much better than the classical description. We have plotted the derivative of scale factor with time in Fig. 9, which shows that time variation of scale factor as computed from effective theory agrees well with the change of the expectation values of scale factor in the regimes before and after the peak. In particular, the inflationary behavior in the modified region with increasing $\dot{a}$ can be seen from the effective semiclassical as well as the quantum solution. After the peak, both show the expected noninflationary behavior.

Interestingly, around the peak the effective classical time derivative is larger than the change in expectation values,

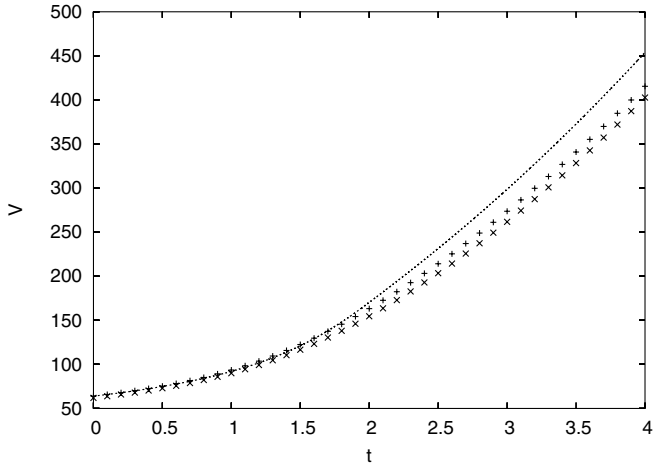


FIG. 8. Volume expectation values (+ for $\langle\hat{V}\rangle$ and × for $\langle\hat{a}\rangle^3$) compared to the effective classical solution (dashed curve). Compared to the points in Fig. 4 the quantum behavior is different since the initial wave packet is now peaked on the effective rather than unmodified classical constraint surface (which decreases the initial $c_0$).

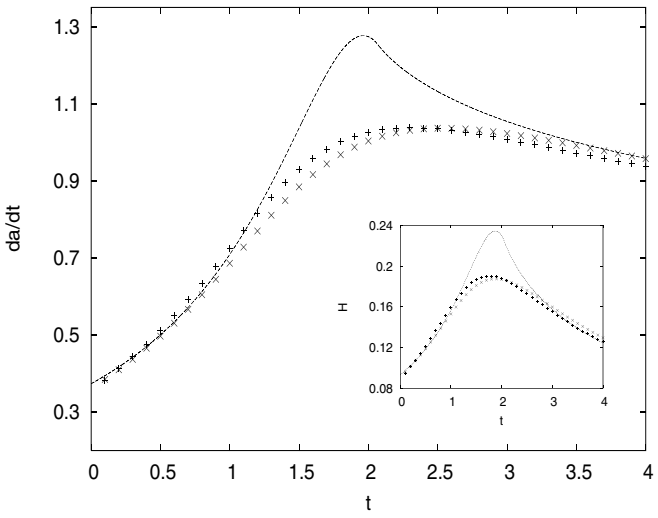


FIG. 9. Time derivative of scale factors plotted in Fig. 8. The inset shows variation of Hubble rate with time ($H = \dot{a}/a$).

which is also the reason why the effective classical volume is slightly larger than the quantum volume at later times in Fig. 8. At the point where the peak occurs, $\dot{a}$ is largest so that higher order corrections (higher powers of $\dot{a}$ in the Friedmann equation) are expected to have the strongest influence. Those corrections have not yet been included into effective semiclassical equations, and we leave a more detailed investigation of their effect around the peak for future work. Nevertheless, one can see numerically that in the case studied here the effect of higher order terms is negligible. This can also be seen from the fact that those higher order terms arise as powers in $c = -\frac{1}{2}\gamma\dot{a}$ which, thanks to the smallness of $\gamma$, remains sufficiently small compared to one throughout the evolution. Moreover, for the flat model the Hamiltonian is invariant under change of sign in $c$ such that the next higher order correction is suppressed by a power $c^2$.

Rather, the reduced derivative of the scale factor around the peak is a consequence of deformations of the wave packet as shown in Fig. 10. In fact, around the peak the effective density changes rather rapidly from increasing to decreasing behavior. Thus, a part of the wave packet will already be in the decreasing regime while its center is still in the increasing one, which lowers the overall density seen by the wave. This behavior is verified by looking at the skewness of the wave packet during the evolution, which is plotted in Fig. 10. First, the skewness turns positive which means that the right tail of the wave packet becomes heavier than the left one. At some point, skewness starts to decrease and reaches negative values, describing a redistribution of parts of the wave packet such that now the left tail becomes more pronounced. This redistribution implies that expectation values of powers of $m$, such as the scale factor and volume, are lowered as compared to the expected evolution. In fact, comparing Fig. 10 with Fig. 9 shows that the turnaround of skewness starts just

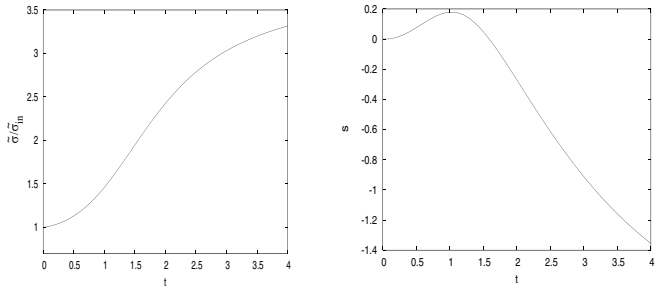


FIG. 10. The time variation of standard deviation and skewness for dust with effective density modification.

when the deviations between the change of $\langle\hat{a}\rangle$ and the effective $\dot{a}$ appear, with the expectation values increasing less strongly than the effective classical value.

This observation shows that effective classical equations used so far do not capture all details in the quantum evolution around the peak. On the other hand, the behavior before and after the peak is described very well. Cosmological studies so far have mainly focused on the modified behavior at small-scale factors and the initial inflationary epoch, which is modeled reliably by using just the effective density. The peak behavior was actually more problematic since the Hubble parameter in the case of scalar dynamics easily became dangerously high, larger than 1 in terms of Planck units, which leads to doubt in the further semiclassical evolution. Here, the quantum behavior with smaller $\dot{a}$ suggests that additional effects from the wave packet can lead to a better semiclassical picture, which may be modeled in effective classical equations by taking into account effects of skewing wave packets. How this appears in the case of a scalar field, and whether in this case $\dot{a}$ can become large enough for higher order corrections to be relevant, remains to be studied.

### 3. Bounces

So far we have looked at only the evolution for rather large volume. For smaller $|m|$, the approximation by classical evolution will become worse and eventually break down. When exactly this is happening depends on the parameters for the cosmological model and the choice of initial wave function. As an example we again use the dust model but evolve to earlier times, towards the classical singularity. In Fig. 11 we show the evolution of the wave packet as it deforms once a significant part of it reaches $m = 0$. As in the case of dust we first compare volume expectation values obtained from (15) with the classical theory. The result is shown in Fig. 12, which shows a bounce at nonzero volume for expectation values. The classical curve first hits the singularity at zero volume.

It should be noted that the effective classical equations of a flat model do not allow a bounce even when we use the effective density in the dust case, and thus this bounce is not of the semiclassical type as in [13–17]. Further, deformations of the wave function show directly that the clas-

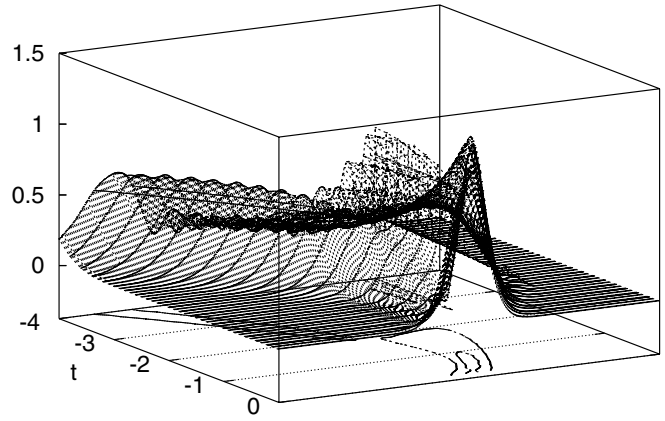


FIG. 11. Wave packet evolving toward the classical singularity and bouncing off, only penetrating negligibly to negative $m$ (to the right). The parameters are $m_c = 100$, $N = 500$, $\sigma = 10$, $M = 10$, $j = 200$.

sical space-time picture is not valid during the bounce phase. Moreover, the nature of a wave packet as opposed to sharp classical values becomes more relevant, which provides a quantitative explanation of the observed bounce. The spread $\sigma$ implies a correction to the Friedmann equation which then takes the form [25]

$$\dot{a}^2 + \tfrac{1}{4}\gamma^{-2}\sigma^{-2} = \tfrac{2}{3}a^2\rho(a), \tag{26}$$

where for simplicity we ignore the $a$ dependence of $\sigma$ due to spreading. Using the small-$a$ expansion (25) for $d_j(a)$ in $\rho(a) = Md_j(a)$ and setting $\dot{a} = 0$ for the bounce results in a bouncing scale factor (in Planck units)

$$a_{\text{bounce}} \sim 3^{-25/28}(\tfrac{7}{4})^{3/7}(\tfrac{1}{8}\sigma^{-2}M^{-1}\gamma^{11/2}j^{15/2})^{1/14} \approx 2.44. \tag{27}$$

Since we used the small-$a$ expansion, which overestimates $d_j(a)$, the bounce value is slightly larger resulting in $a_{\text{bounce}} \approx 2.50$ if the function $d_j(a)$ is used in its full form. The corresponding bounce volume $V_{\text{bounce}} \approx 15.6$ is considerably smaller than the minimum expectation value in Fig. 12. But if we use the effective Friedmann equation (26) to place the initial wave packet on the effective constraint surface the expected bounce radius and the numerical one in Fig. 13 agree within the limits of the expectation values $\langle\hat{V}\rangle$ and $\langle\hat{a}\rangle^3$. In fact, the wave packet bounces earlier than expected, but around the expected volume. Thus, the spread-dependent correction term explains why there is a bounce and gives a good estimate for the bounce radius.

Nevertheless, it is also clear from Fig. 13 that the agreement between the expectation values and the effective solution deteriorates around the bounce. This can also be seen from Fig. 14, which shows considerable change in spread of the wave function. In fact, the wave packet does not only spread but also separates into different packets, as seen in Fig. 15. Thus, even taking into account the spread dependence in the modified Friedmann equation would not completely describe the quantum behavior. (Note that the spread-dependent correction term was derived under the assumption of a Gaussian wave packet. Figure 14 also shows that the skewness does not increase strongly, but for this case of a wave separating into different packets skewness alone is not a good measure for the deviations from a Gaussian.) The evolution can then no longer be seen as semiclassical and it is not possible to get a better agreement by including further corrections into an effective equation.

Still, one can also see that there is a rather undisturbed wave packet bouncing off, while other parts of the wave function stay around the classical singularity which does

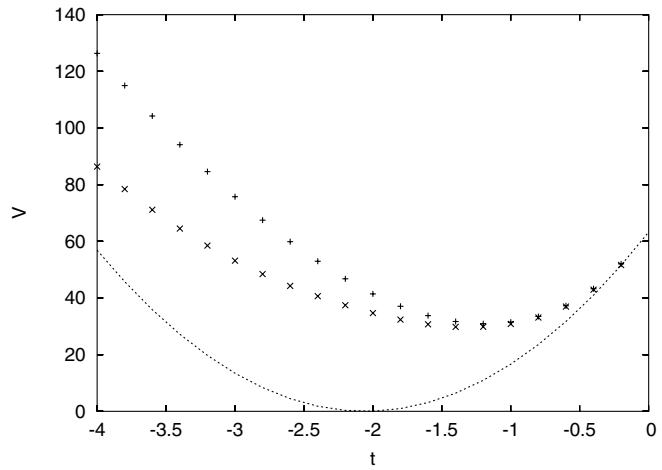


FIG. 12. Volume expectation values for the wave packet in Fig. 11. The expectation values bounce at nonzero values, while the classical curve hits zero volume.

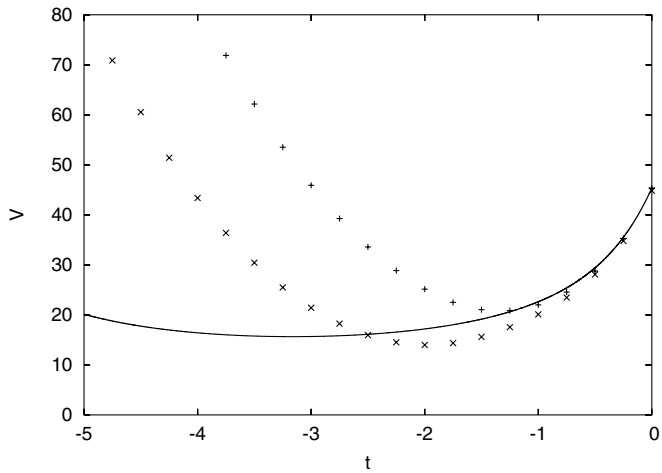


FIG. 13. Volume expectation values for the wave packet initially peaked at the effective constraint surface compared to a numerical solution (solid curve) of the effective Friedmann equation (26). Since the corresponding wave packet, plotted in Fig. 15, moves closer to the classical singularity than in Fig. 11, the spread of wave function increases faster than in Fig. 12.

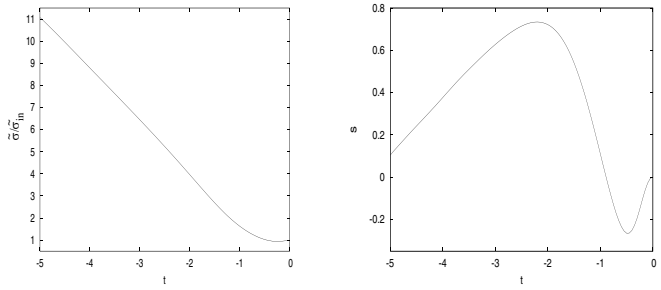


FIG. 14. Increase in spread and skewness for backward evolution through a bounce as in Fig. 13.

not affect expectation values of geometrical quantities very much. Thus, during the evolution shown here the expectation value of the volume and the cube of that of the scale factor do not deviate too much near the classical singularity. However, since strong oscillations build up rapidly, there are strong curvature fluctuations. This is shown in Fig. 16, where the fluctuations of $\dot{a}$, computed from the operator

$$(\hat{\dot{a}}\psi)_m = \tfrac{1}{2} i \gamma^{-1} (\psi_{m+1} - \psi_{m-1}), \tag{28}$$

which initially are smaller than $\dot{a}$, increase to have a maximum at the bounce. After the bounce, curvature fluctuations decrease but stay larger than initially, and are comparable to the value of $\dot{a}$ in Fig. 17. We thus can still think of semiclassical spatial slices of a certain volume at least in early stages of the bounce, but since the extrinsic curvature is not sharp, one cannot think of them as forming a classical, smooth space-time.

If, as before, we compute the time derivative of the expectation value of the scale factor, rather than the expectation value of curvature, it is seen from Fig. 17 that it is still increasing. That is, it accelerates, as a consequence of the effective density. This figure also shows that the expectation value of the $\dot{a}$ operator (28) follows the change of

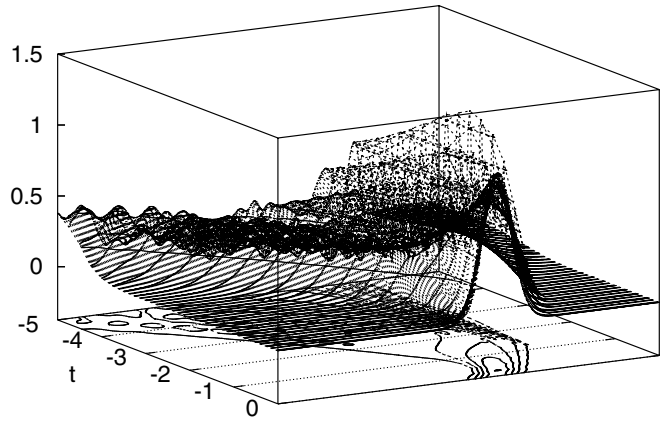


FIG. 15. Wave packet evolving toward the classical singularity and bouncing off as in Fig. 11, but initially peaked on the effective constraint surface at $m_c = 80$. Since the bounce radius now is smaller, the leakage to negative $m$ is larger (see rightmost contour line).

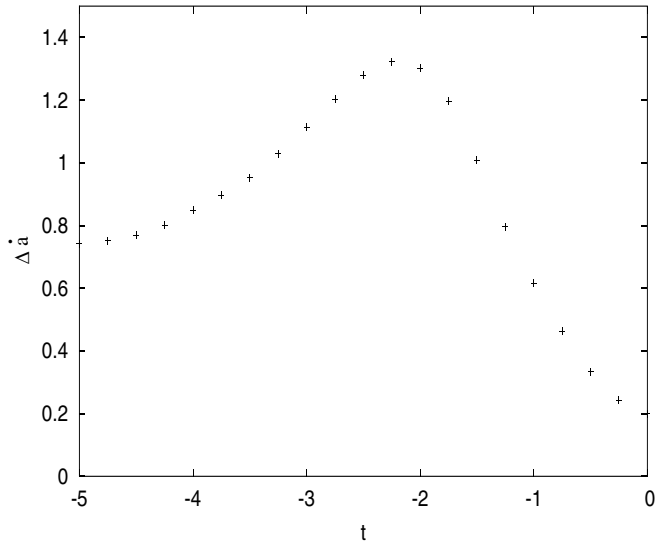


FIG. 16. Extrinsic curvature fluctuation $\Delta\dot{a} = \sqrt{\langle(\hat{\dot{a}})^2\rangle - \langle\hat{\dot{a}}\rangle^2}$ corresponding to Fig. 13 where the operator for $\dot{a}$ is derived from the $c$ operator mapping a state $\psi_m$ to $\frac{1}{4} i(\psi_{m+1} - \psi_{m-1})$.

$\langle\hat{a}\rangle$ more closely than the effective classical solution, which implies that the interpretation of extrinsic curvature (computed from the geometrical quantity $a$ as compared to connection components) has an unambiguous meaning.

As seen in Fig. 15, the wave function leaks only slightly into the part of minisuperspace corresponding to negative $m$ (i.e., the part corresponding to the side beyond the classical singularity in the internal time formulation [8,48]). This is another reason for the fact that we can still approximately speak of a classical bounce of the volume. If the wave function at negative $m$ would be larger, also the spread in spatial geometrical quantities and not just in extrinsic curvature would be large and classical geometry would break down completely. Whether or not this is happening depends very sensitively on detailed quantiza-

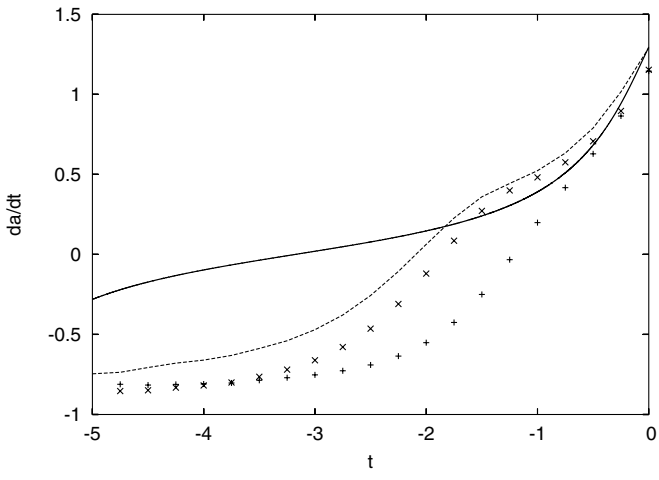


FIG. 17. Time derivative of the scale factor expectation values in Fig. 13 compared to the effective solution (solid curve). The dashed curve connects expectation values $\langle\hat{\dot{a}}\rangle$.

tion choices in the Hamiltonian constraint and initial values of the wave function (see also [38,41,49]).

## V. CONCLUSIONS

Splitting group averaging into two steps, first evolving an initial state and then integrating along the group orbit, allows us to introduce a coordinate time parameter into quantum gravity, although only in an approximate sense. The resulting time-dependent family of states, the state-time, does not solve the constraint exactly; only integrating over time results in a physical state. Moreover, this does not introduce a physical time parameter into the quantum theory, but only coordinate time in semiclassical regime. Still, the resulting evolution equations are helpful in semiclassical analysis and in providing intuitive pictures of quantum effects.

Our main application in this paper is a justification of using effective densities as the most prominent quantum gravity effect imported into effective classical equations. As it turns out, the modified classical equations describe the quantum evolution of wave packets very well, down to surprisingly small scales. Stronger deviations become noticeable only when the wave packet starts to touch the classical singularity. When exactly this happens depends on details of the model and the chosen initial state. The diverse effects giving rise to departures from classical behavior can be separated by varying the parameters involved in the models. For instance, we chose rather large values for the ambiguity parameter $j$ determining the peak of the effective density, in order to distinguish this effect from that of perturbative corrections. In this way it is possible to study each correction term in the effective Hamiltonian separately.

The replacement of classically diverging factors of $a^{-3}$ in dynamical equations by a bounded effective density $d_{j,l}(a)$ has been confirmed as the main effect. Effective densities themselves are partly responsible for this observation since, via the effective Friedmann equation, they lead to a reduction of extrinsic curvature $\dot{a}$. This means that higher order corrections, i.e., higher powers of $\dot{a}$, are less relevant at small $a$ than without effective densities. Visible effects then occur most likely around the peak of the effective density, where $\dot{a}$ is largest. As observed here, the quantum Hubble rate is in fact smaller than would be expected just from the effective density, which is helpful for cosmological applications. However, numerically one can check that in the cases studied here the reduced Hubble rate is a consequence of deformations of the wave packet, parametrized here by the skewness, rather than of higher order terms. Such an effect would have to be included in effective classical equations by introducing a correction term depending on the skewness of an evolving wave packet. That it is possible to describe the influence of properties of wave packets on the evolution by effective classical equations has been demonstrated here by studying bounces implied by a spread-dependent correction term. The corresponding correction for skewness, however, is not known since in the derivations of correction terms so far Gaussian states with zero skewness have been used [25]. For cosmological purposes it would be interesting to apply this technique to the case of a scalar field and study the role played by effective densities, in particular, around the peak.

Detailed formulas for perturbative correction terms, which include higher order and higher derivative corrections, and uncertainty correction terms related to the spread of the wave function, are currently being evaluated. Once available, they can be used for a direct comparison with the quantum evolution as studied here. In particular, the uncertainty corrections, which are proportional to $\sigma^{-2}$ [25], play a role at small volume since, unlike higher order corrections, they are not suppressed by effective densities. An application of this correction term can be found in studying bounces, where it provides an explanation for the bounce in Fig. 11 which does not follow from effective densities alone. The expression (27) of the bounce radius determines the scale where quantum effects from the wave packet become important, indicated by correction terms depending on the spread $\sigma$. For a phenomenological analysis, $a_{\mathrm{bounce}}$ can be used as initial value of the scale factor, which is relevant for estimates of the amount of inflation. Since the value derived here for dust depends on all the parameters of the model, in particular the ambiguity parameter $j$, it is clear that the analysis will be more complicated than the original ones, where the initial scale factor was assumed to be $a_{\mathrm{initial}} = \sqrt{\gamma}\ell_{\mathrm{P}}$. With an expression like $a_{\mathrm{bounce}}$, more reliable estimates can be made and constraints on the parameters can be tightened. Thanks to the strong initial increase of $d(a)$ with $a$, which is responsible for the small power $1/14$ in (27), the dependence on parameters of the model is, fortunately, rather weak.

At very small scales the evolution of wave packets shows when the classical space-time picture can be trusted, when it needs to be corrected, and when it breaks down completely. In this regime the evolution becomes much more sensitive to quantization choices in the Hamiltonian constraint. In particular, this is true for the leakage into the domain of negative $m$, where the orientation of space is reversed, which is not surprising since this corresponds to evolution beyond the classical singularity in the internal time picture. In this context one should note that we had to use a symmetric ordering of the constraint for the coordinate time evolution to be numerically stable. This ordering already implies changes to the issue of initial conditions [50,51] and on the relation between the wave function at positive and at negative $m$. The alternative procedure of using a lapse function $N(t) = a(t)$ and quantizing $NH$ symmetrically, as mentioned in Sec. IVA, also changes the issue of initial conditions since the lapse vanishes at the classical singularity and the wave function at negative $m$

completely decouples from that at positive $m$. Thus, while the coordinate time picture is well suited to justifying effective classical equations at nonvanishing volume, the issue of the classical singularity can be understood only by using the wave function directly and thus employing an internal time to formulate evolution. Since the classical space-time picture breaks down in this regime, there is no analog to coordinate time.

## ACKNOWLEDGMENTS

We thank Kevin Vandersloot for useful discussions. P. S. thanks Max-Planck-Institut für Gravitationsphysik for supporting a visit and warm hospitality during the early stage of this work. His work is supported in part by Eberly research funds of Penn State and by NSF Grant No. PHY-00-90091.

[1] M. Bojowald and H. A. Morales-Técotl, in *Proceedings of the Fifth Mexican School (DGFM): The Early Universe and Observational Cosmology*, Lecture Notes in Physics Vol. 646 (Springer-Verlag, Berlin, 2004), pp. 421–462.
[2] M. Bojowald, in *Proceedings of the International Conference on Gravitation and Cosmology (ICGC 2004), Cochin, India* [Pramana 63, 765 (2004)].
[3] M. Bojowald, Phys. Rev. Lett. **89**, 261301 (2002).
[4] M. Bojowald and K. Vandersloot, Phys. Rev. D **67**, 124023 (2003).
[5] M. Bojowald, G. Date, and K. Vandersloot, Classical Quantum Gravity **21**, 1253 (2004).
[6] G. Date and G. M. Hossain, Classical Quantum Gravity **21**, 4941 (2004).
[7] M. Bojowald, Classical Quantum Gravity **18**, 1071 (2001).
[8] M. Bojowald, Classical Quantum Gravity **19**, 2717 (2002).
[9] M. Bojowald, Classical Quantum Gravity **20**, 2595 (2003).
[10] S. Tsujikawa, P. Singh, and R. Maartens, Classical Quantum Gravity **21**, 5767 (2004).
[11] M. Bojowald *et al.*, Phys. Rev. D **70**, 043530 (2004).
[12] G. Date and G. M. Hossain, gr-qc/0407069.
[13] P. Singh and A. Toporensky, Phys. Rev. D **69**, 104008 (2004).
[14] J. E. Lidsey, D. J. Mulryne, N. J. Nunes, and R. Tavakol, Phys. Rev. D **70**, 063521 (2004).
[15] G. V. Vereshchagin, J. Cosmol. Astropart. Phys. 07 (2004) 013.
[16] M. Bojowald, R. Maartens, and P. Singh, Phys. Rev. D **70**, 083517 (2004).
[17] G. Date and G. M. Hossain, gr-qc/0407074 [Phys. Rev. Lett. (to be published)].
[18] M. Bojowald and G. Date, Phys. Rev. Lett. **92**, 071302 (2004).
[19] M. Bojowald, G. Date, and G. M. Hossain, Classical Quantum Gravity **21**, 3541 (2004).
[20] P. G. Bergmann, Rev. Mod. Phys. **33**, 510 (1961).
[21] K. V. Kuchař, in *Proceedings of the 4th Canadian Conference on General Relativity and Relativistic Astrophysics, Winnipeg, Manitoba, 1991*, edited by G. Kunstatter, D. E. Vincent, and J. G. Williams (World Scientific, Singapore, 1992).
[22] C. Rovelli, Phys. Rev. D **43**, 442 (1991).
[23] D. Marolf, gr-qc/9508015.
[24] A. Ashtekar, M. Bojowald, and J. Lewandowski, Adv. Theor. Math. Phys. **7**, 233 (2003).
[25] A. Ashtekar, M. Bojowald, and J. Willis (work in progress).
[26] A. Ashtekar *et al.*, J. Math. Phys. (N.Y.) **36**, 6456 (1995).
[27] T. Thiemann, Classical Quantum Gravity **15**, 839 (1998).
[28] T. Thiemann, Classical Quantum Gravity **15**, 875 (1998).
[29] T. Thiemann, Classical Quantum Gravity **15**, 1207 (1998).
[30] T. Thiemann, gr-qc/0305080.
[31] J. Lewandowski and D. Marolf, Int. J. Mod. Phys. D **7**, 299 (1998).
[32] R. Gambini, J. Lewandowski, D. Marolf, and J. Pullin, Int. J. Mod. Phys. D **7**, 97 (1998).
[33] M. Bojowald and H. A. Kastrup, Classical Quantum Gravity **17**, 3009 (2000).
[34] M. Bojowald, Phys. Rev. D **64**, 084018 (2001).
[35] M. Bojowald, Classical Quantum Gravity **19**, 5113 (2002).
[36] T. Thiemann, Classical Quantum Gravity **15**, 1281 (1998).
[37] M. Bojowald and F. Hinterleitner, Phys. Rev. D **66**, 104003 (2002).
[38] F. Hinterleitner and S. Major, Phys. Rev. D **68**, 124023 (2003).
[39] M. Bojowald and G. Date, Classical Quantum Gravity **21**, 121 (2004).
[40] D. Cartin, G. Khanna, and M. Bojowald, Classical Quantum Gravity **21**, 4495 (2004).
[41] D. Green and W. Unruh, Phys. Rev. D **70**, 103502 (2004).
[42] M. Domagala and J. Lewandowski, Classical Quantum Gravity **21**, 5233 (2004).
[43] K. A. Meissner, Classical Quantum Gravity **21**, 5245 (2004).
[44] A. Ashtekar, J. C. Baez, A. Corichi, and K. Krasnov, Phys. Rev. Lett. **80**, 904 (1998).
[45] A. Ashtekar, J. Baez, and K. Krasnov, Adv. Theor. Math. Phys. **4**, 1 (2000).
[46] J. M. Velhinho, Classical Quantum Gravity **21**, L109 (2004).
[47] G. M. Hossain, Classical Quantum Gravity **21**, 179 (2004).
[48] M. Bojowald, Phys. Rev. Lett. **86**, 5227 (2001).
[49] M. Bojowald and K. Vandersloot, gr-qc/0312103.
[50] M. Bojowald, Phys. Rev. Lett. **87**, 121301 (2001).
[51] M. Bojowald, Gen. Relativ. Gravit. **35**, 1877 (2003).